



Presenting three design methods for axial compressor blade via optimization

Omid Fathi^a, Hadi Kargarsharifabad^{a,b,*}

^aDepartment of Mechanical Engineering, Najafabad Branch, Islamic Azad University, Najafabad, Iran.

^bEnergy and Sustainable Development Research Center, Semnan Branch, Islamic Azad University, Semnan, Iran

Article info:

Received: 30/09/2016
Accepted: 10/01/2018
Online: 10/04/2018

Keywords:

Parametric geometry,
Loss coefficient,
Optimization algorithm,
Multi-point objective
function.

Abstract

Improving the efficiency of compressors has been one of the most important goals of researchers over the years. In this paper, three different methods are presented for parameterization and blade optimization of axial flow compressor. All methods consist of flow analysis tool, optimization algorithms, and parametric geometry generation tool that are different in each approach. An objective function is defined based on the aerodynamic performance of blade in the acceptable incidence angles range. A double circular arc blade is used as the initial guess for all methods. The performance of optimized blades and the initial blade are compared to evaluate the capability of various methods, and a good agreement is achieved. The results show that the level of performance improvement in each method depends on the number and type of the chosen parameters. All three methods have improved blade performance at the design incidence angle. However, only the first method shows significant performance improvement in off-design conditions.

Nomenclature

Blade chord	c	Angle of the suction surface	μ
Length	L	Edge angles of leading and trailing	χ
Height control points	n	Loss coefficient	ω
Distance control points of the leading edge	t	Subtitles	
The weight of the objective function	W_i	Different length indicator	1,2,3,4
Coordinates x	x	The average value	Ave
Coordinates y	y	Coefficient	coef
Greek signs		Exit	e
The angle of attack	α	Leading edge Parameters	l
Input	i	Installation angle	γ
Interval changes the angle of attack	$\Delta\alpha$	Minimize loss	min
		Reference values	ref

1. Introduction

The axial compressor is one of the largest power consumers in industries. For example, the

compressor in a gas turbine consumes more than 50 percent of the generated power. Therefore, improving the efficiency of compressors has been one of the most important goals of researchers over

the years. Aerodynamic optimization is an important factor in compressor efficiency enhancement.

Nowadays, different methods of optimal design, including aerodynamic design, have brought about many improvements in the operation of axial compressors. In general, the aerodynamic design of axial compressors aims at increasing efficiency, raising pressure ratio, widen operational range, and increasing surge margins. Each goal has different effects on the configuration of the compressor. In this regard, a great deal of research has been conducted to develop optimized methods for blade design using numerical algorithms. Adopting a geometrical production tool along with an optimization method and a tool for fluid dynamic analysis of the flow are typical options in the optimal design of compressor blades.

Park et al. [1] presented three-dimensional measures of a one-row blade. Bonaiuti and Zangeneh [2] presented a strategy for multiple-point and multiple-purpose three-dimensional optimization of turbo-machinery blades. This strategy was developed based on the reverse design of the blade; they integrated response surface optimization, multi-objective evolutionary algorithm, and computational fluid dynamics analysis. Korakanites [3] presented a method for the direct design of the blade aiming at enhancing the capability of two-dimensional geometry production of the blade. This method is used to produce input blade in direct or reverse design in subsonic and supersonic circumstances for turbine and compressor. This procedure improves aerodynamic and heat transfer operation of the blade. Many researchers such as Sonoda and et al. [4], Shahpar and Rodford [5], Kammerer and et al. [6], Buche and et al. [7], Benini and Tourlidakis [8], Bonaiuti and Pediroda [9] conducted many activities to reduce the computational costs of the numerical design of the blade. Siddappaji et al. [10] presented a new multi-dimensional method that consists of low-level optimizations of the thorough flow and used empirical relations to estimate performance. Their method is only valid for preliminary design and the design using conventional blades. Jaron et al. [11] presented a new method for optimizing blade of the

compressor for reducing noise on trailing edge. Vitale et al. [12] developed a new adjoint solver for non-ideal compressible flow method for designing compressor blade.

Turbo-machinery designs are usually multi-dimensional problems in which different parameters should be considered in the design process. Multi-objective optimizations require a lot of simulations. Therefore, the use of automatic methods for blade design is limited due to high computational costs. This problem becomes acuter when operational parameters are calculated at multiple operational points. Hence, several simulations are carried out to estimate the performance of a blade.

In this study, three different methods are presented for parameterization and multiple-point optimization of compressor blades, as well as the ability and computational costs of these methods in achieving the designer's desired objectives, are compared.

2. Problem description

Fig. 1 shows the results of stream line curvature analysis in a 16-stage axial compressor. The value of the angle of attack and profile loss in each row of the blade are displayed for 6 different working points (one point close to stall, one point close to choke, and one point between choke and stall in revolutions equal to 100% and 70% of nominal revolution). The changes of the angle of attack in the first rotor are approximately 20° , in middle stage approximately 10° , and 40° in rear stages. Similarly, the loss value in middle stage is about 20%, and it reaches 10% in rear stages. As a rule in designing for this compressor, it is seen that the middle stage does not have considerable changes in the angle of attack. Therefore, the designer's focus should be on reducing the value of loss in the design angle. In case of the front and rear stages, the changes of the angle of attack are significant. Therefore, the designer should direct at designing blades that have less sensitivity to change in the angle of attack.

Fig. 2 shows the loss variation graphs in term of the angle of attack of a sample blade. In this diagram, the value and the place of minimum loss and the range of change of the attack angle

from stall to choke are shown. In general, optimization is carried out to increase $\Delta\alpha$ and reduce ω_{min} in a certain α_{min} . By increasing the loading of the blades, the minimum value of loss increases, and the value of $\Delta\alpha$ decreases. In cases where there are not many changes in off-designs, the design can be done aiming at reducing the minimum loss, and in cases where the changes of the angle of attack in off-design circumstances are huge, design can be done aiming at increasing $\Delta\alpha$. Eq. (1) shows the proposed objective function to design the blade in this study.

$$O.f = W_1 \times \frac{\omega_{min}}{\omega_{min.ref}} + W_2 \times \frac{|\alpha_{min.ref} - \alpha_{min}|}{\alpha_{min.ref}} + W_3 \times \frac{\Delta\alpha_{ref}}{\Delta\alpha} \quad (1)$$

where the values with the ref subscripts are the values obtained from the middle pass flow of the compressor. W_i is the weight of each term of the objective function. The designer applies the philosophy of the blade design to the design tool using these weights.

The computational cost of the above objective is high because the calculation of equation parameters need cascade fluid analysis of the blade in a few different points.

3. Optimization process

In this research, the direct method is used to design the blade. In this procedure, the designer gives the geometry as input to flow analysis code and receives the operation of the blade as output. The blade performance can play a guiding role for decreasing and increasing the loads applied and to decide how to improve blade surface. In reverse or quasi-reverse methods, pressure distribution or Mach number should be determined on the blade surface. Given that appropriate Mach number and pressure distribution corresponding to

the design, the objective is unclear, and using these methods in the mentioned design system requires an extra design loop to determine the appropriate distribution of pressure or Mach number on the blades.

Therefore, in this study, a completely direct method is used. In the direct method, the geometry of the blade is expressed in parametric form, and these parameters are optimized based on the objective function expected by the designer. Different methods of parameterization of the blade geometry have a great impact on the time and quality of compressor blade optimization. In this research, three different methods of blade design are presented, and they are compared to each other in terms of optimization time and quality.

Fig. 3 shows the optimization algorithm used in this paper. In this method, a gradient-based method is used for blade optimization. At first, the geometry of a blade is given to the optimization system of the blade as the input. Via a re-parameterization process, suitable parameters for the basic geometry are generated. These parameters enter the optimization process as the initial guess. In the re-parameterization process, different parameters are calculated in a way that the geometry resulting from these parameters and the initial geometry have the least deviation. In addition to the coordinates of points, to calculate deviation, the slope and curvature of curves are compared at different points. In the optimization process, the initial geometry changes in a way that the objective function of Eq. (1) reaches its least value. Parameters of tangential distance between blades (S/C), installation angle, lift coefficient (the proportion of tangential forces to the output dynamic head), and the maximum thickness (the least maximum thickness is applied to the optimization process as a structural constraint) are achieved through mean line thorough flow design of the compressor and structural limitations.

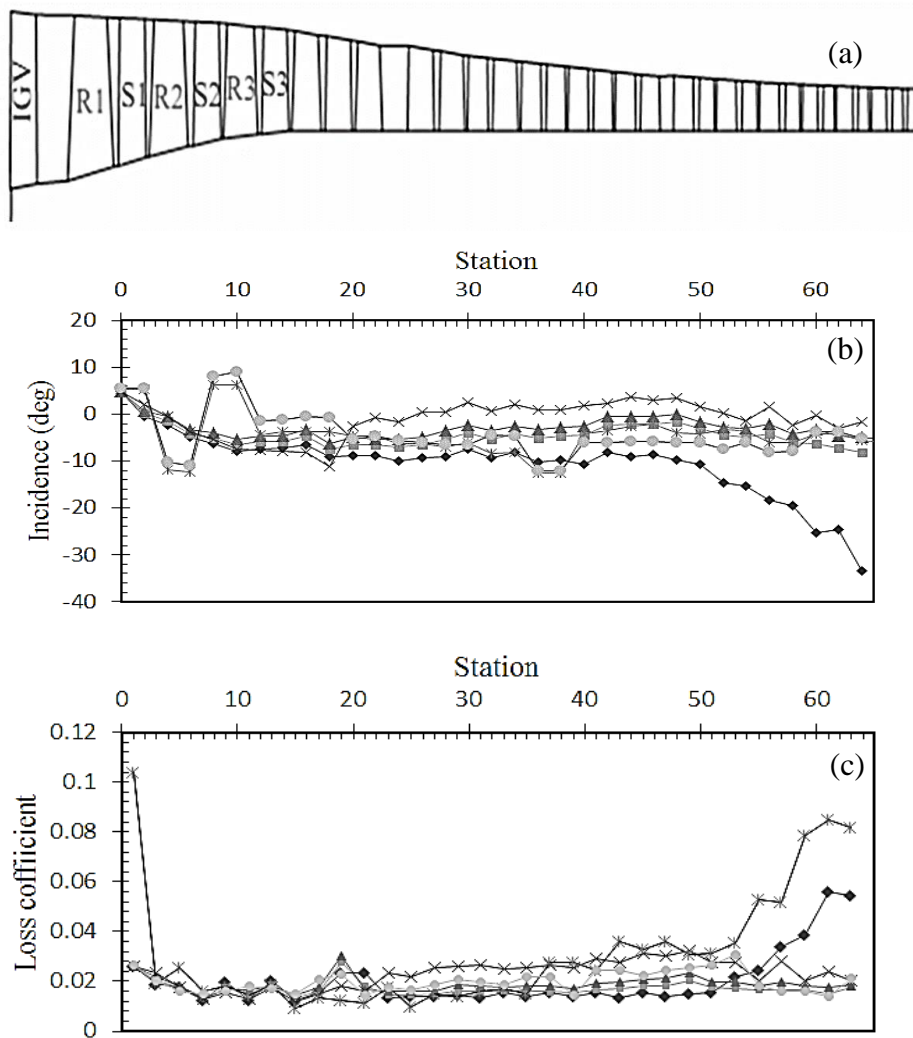


Fig. 1. (a) 16-stage axial compressor, (b) incidence angle and (c) profile loss at mean line [13].

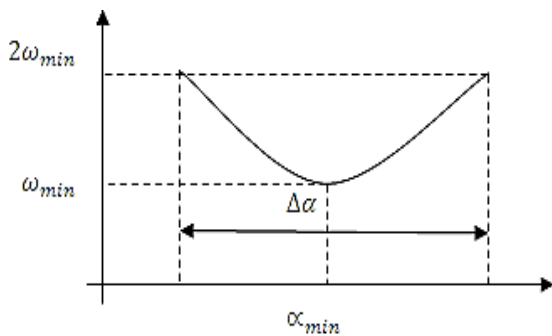


Fig. 2. Loss variation versus incidence angle [13].

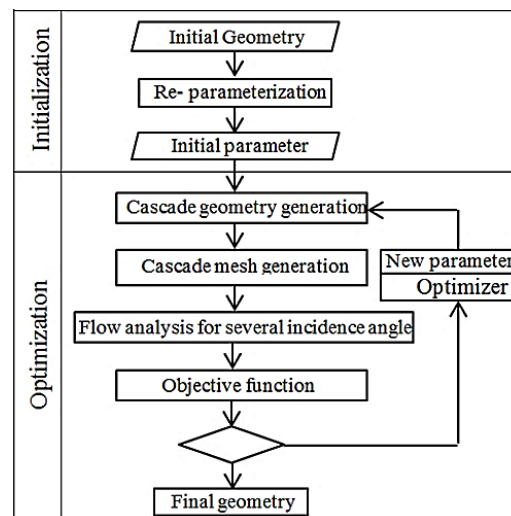


Fig. 3. Blade optimization process.

3.1. Geometry parameterization methods

An appropriate design system requires a tool which can produce a suitable geometric model of a blade in addition to high flexibility with the least number of parameters. Thru increasing the loading of the compressor blade, due to a rise in the negative pressure gradient, the value of minimum drop increases and the gradient of drop variations decreases in proportion to the angle of attack. Therefore, the designer must strike a balance between the load of the blade, the minimum value of decline and the variation range of the angle of attack. The more flexible the parametric geometry of the production method, the higher the possibility of designing a blade with better flow control. On the other hand, the increase in the number of parameters means a rise in time and calculation costs of the blade design. In each method, two-dimensional geometries of a blade are defined by four curves: leading and trailing edges and pressure and suction surfaces. Leading edges in each of the three methods are defined by the arc of a circle. A shape function, Eq. (2), is also added which causes the value of the curvature of leading edge to change so by an increase in the value of α , the value of the angle of attack decreases (the leading edge become more beveled). Fig. 4 shows a leading edge and the parameters used to define it. In all three methods, trailing edge is defined by a semi-circle. The semi-circle diameter is one of the constructional limitations which should not become less than the allowable minimum value in the entire optimization process.

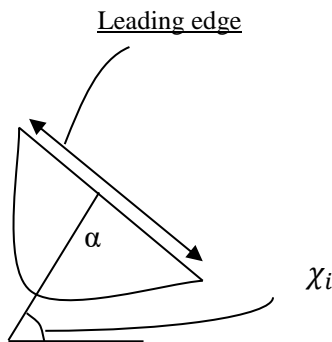


Fig. 4. Geometric parameterization of leading edge.

Therefore, the only parameters that enter the optimization process are the angle of trailing edge and its thickness (Eq. (2)).

$$f(x) = (x \times (1 - x))^\alpha \quad (2)$$

$$0 < \alpha < 1$$

Fig. 5 shows the geometry of the trailing edge and the parameters used to define it. There are three different methods to define suction and pressure surfaces in different blade optimization methods. In the first method, the suction surface is defined by an 8-point Bezier curve. The 1st and 8th points are achieved through the geometry of the leading and trailing edges.

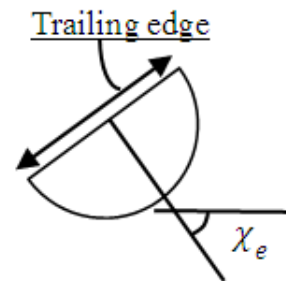


Fig. 5. Geometric parameterization of trailing edge.

The coordinates of the 5th and 6th points are among design parameters. The coordinates of the 2nd, 3rd, 6th, and 7th points, assuming that the curve and rigidity of the curve (Eqs. (3 and 4)) are known, are calculated at the beginning and the end of the intake surface. Fig. 6 shows the geometry and the parameters used to define the suction surface in the first method.

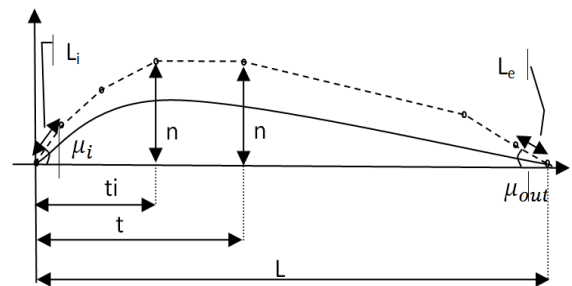


Fig. 6. Geometry and parameters used of suction surface in the first method.

The number of parameters in this method is large; however, due to the close relationship of the curvature (k) and rigidity of surfaces with cascade flow pattern, this method brings about an improvement in the optimization speed.

$$\kappa = \frac{(\dot{x}\ddot{y} - \dot{y}\ddot{x})}{(\dot{x}^2 + \dot{y}^2)^{3/2}} \quad (3)$$

$$stiffness = \frac{(\dot{x}\ddot{x} + \dot{y}\ddot{y})}{(\dot{x}^2 + \dot{y}^2)} \quad (4)$$

In the second method, suction surface is defined by couple of two-point Bezier curves, one from the attack edge up to the maximum thickness place and the other, from leading edge to the maximum thickness place. The coordinates of the initial and final points of the suction surface are obtained through leading edge and trailing edge surfaces curves, and the coordinates of other points are defined as parameters; they are considered to be the same at the junction of the slope and the curvature of two curves. Fig. 7 shows the geometry and the parameters used to define the suction surface using the second method.

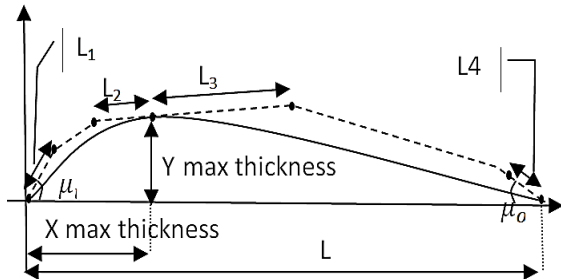


Fig. 7. Geometry and parameters of suction surface in the second method.

The great number of parameters in the two mentioned methods increases the computational costs of blade design. Fig. 8 shows the geometry and the parameters used to define the blade in the third method. The suction surface in the third method is defined by a four-point Bezier curve. In this method, the coordinates of the 1st and the 4th points of the Bezier curve are obtained from the geometry of the leading and trailing edge surfaces. Therefore, only the coordinates of the 2nd and 3rd points have a role in defining suction surface as a design parameter. Given the low number of parameters

in this method, optimization costs are lower, but the flexibility of this method is also lower than the former. The pressure surface in the first method is defined by a 5-point Bezier curve. However, in the second and third methods, pressure surface is defined similarly to suction surface.

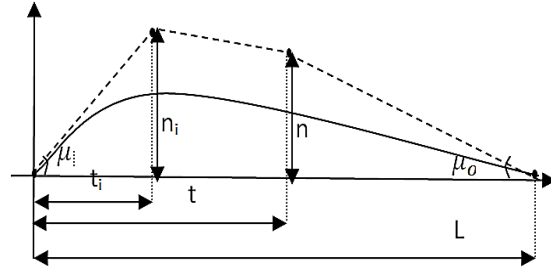


Fig. 8. Geometry and parameters of suction surface in the third method.

3. 2. Flow analysis

Accurate calculations of the cascade loss in different conditions are necessary to determine an objective function. Thus, a flow analysis tool including mesh generation tool as well as computational fluid dynamics solver is used to calculate cascade losses. The flow field is automatically divided into several zones in a way that one structured mesh is used for each zone which is able to make a fine mesh near the walls. A two-dimensional compressible viscous flow code is used to simulate the cascade fluid flow. This code is developed based on Roe scheme, so that it could be used to design transonic blades, too. The method presented by Kermani and Plett [14] is used to solve the fluid equations by the Roe scheme in the computational domain and to give a formula for the Roe's numerical fluxes in generalized coordinates. The fluid governing equations for the viscous, unsteady and compressible flow in generalized coordinates with no body force could be shown as follows:

$$\frac{\partial Q_1}{\partial t} + \frac{\partial F_1}{\partial \xi} + \frac{\partial G_1}{\partial \eta} = \frac{\partial G_{1VT}}{\partial \eta} \quad (5)$$

where Q_1 is the conservative vector, F_1 and G_1 are the inviscid flux vectors, and G_{1VT} is the viscous flux vector. Because of high-speed flow in cascade, all the viscous derivatives along the mainstream of the flow are neglected (thin-layer

approximation). Therefore the governing equation can be discretized as follows:

$$\frac{\partial Q_1}{\partial t} + \frac{F_{1E} - F_{1W}}{\Delta \xi} + \frac{G_{1N} - G_{1S}}{\Delta \eta} = \frac{G_{1VTN} - G_{1VTS}}{\Delta \eta} \quad (6)$$

For the time discretization, the two-step explicit scheme, from the Lax-Wendorff family of predictor-correctors, is used. The inviscid numerical flux F_{1E} based on the Roe scheme is written in generalized coordinates, according to Ref. [14]. The other flux term can be written the same as F_{1E} (Eq. 7).

$$F_{1E} = \frac{1}{2} [F_{1E}^L + F_{1E}^R] - \frac{1}{2} \sum_{k=1}^4 |\hat{\lambda}_E^{(k)}| \delta \omega_E^{(K)} \hat{T}_E^{(k)} \left[\frac{\sqrt{\xi_x^2 + \xi_y^2}}{J} \right]_E \quad (7)$$

In order to obtain the left (L) and right (R) flow conditions, a third order upwind-based algorithm with MUSCL extrapolation strategy [15] is applied to the primitive variables (pressure, velocity components and temperature). For example, at the east cell face of the control volume, E, L and R flow conditions are determined as ($k=1/3$ in this study):

$$q_E^L = q_{j,k} + \frac{1}{4} [(1-k)\Delta_{wq} + (1+k)\Delta_{Eq}] \quad (8)$$

$$q_E^R = q_{j+1,k} - \frac{1}{4} [(1-k)\Delta_{EEq} + (1+k)\Delta_{Eq}]$$

For successful modeling of the turbulent effects on the flow, the $K-\omega$ (SST) method is utilized to incorporate modifications for low-Reynolds number effect, compressibility and shear flow spreading. $k-\omega$ (SST) model consists of a transformation of the $k-\epsilon$ model in the outer region to a $k-\omega$ formulation near the surface by a blending function F_1 . Eqs. (9 and 10) are k and ω of the model, respectively.

$$\frac{\partial(\rho k)}{\partial t} + \frac{\partial}{\partial x_j} (\rho U_j k) = \frac{\partial}{\partial x_j} \left[\left(\mu + \frac{\mu_t}{\sigma k_3} \right) \frac{\partial k}{\partial x_j} \right] + P_k + \beta \rho k \omega \quad (9)$$

$$\frac{\partial(\rho \omega)}{\partial t} + \frac{\partial}{\partial x_j} (\rho U_j \omega) = \frac{\partial}{\partial x_j} \left[\left(\mu + \frac{\mu_t}{\sigma_{\omega 2}} \right) \frac{\partial \omega}{\partial x_j} \right] + (1 - F_1) 2\rho \frac{1}{\sigma_{\omega 2} \omega} \frac{\partial k}{\partial x_j} \frac{\partial \omega}{\partial x_j} + a_3 \frac{w}{k} P_k + \beta_3 \rho \omega^2 \quad (10)$$

In this model, the eddy-viscosity formulation is used by a limiter to consider the transport of the turbulent shear stress (Eq. (11)).

$$q_E^L = q_{j,k} + \frac{1}{4} [(1-k)\Delta_{wq} + (1+k)\Delta_{Eq}]$$

$$q_E^R = q_{j+1,k} - \frac{1}{4} [(1-k)\Delta_{EEq} + (1+k)\Delta_{Eq}] \quad (11)$$

$$\mu_t = \rho \frac{a_1 k}{\max(a_1 \omega, SF_2)}$$

F_2 is a blending function which restricts the limiter to the wall boundary layer. S is an invariant measure of the strain rate. The blending functions are defined based on the distance to the nearest wall and the flow variables by Eqs. (12 and 13).

$$F_1 = \tanh \left(\left(\min \left(\max \left(\frac{\sqrt{k}}{\beta \omega y}, \frac{500\nu}{y^2 \omega} \right), \frac{4\rho k}{CD_{k\omega} \sigma_{\omega} 2y^2} \right) \right)^4 \right) \quad (12)$$

where:

$$CD_{k\omega} = \max \left(2\rho \frac{1}{\sigma_{\omega 2} \omega} \frac{\partial k}{\partial x_j} \frac{\partial \omega}{\partial x_j}, 1.0 \times 10^{-10} \right) \quad (13)$$

$$F_2 = \tanh \left(\left(\max \left(\frac{2\sqrt{k}}{\beta \omega y}, \frac{500\nu}{y^2 \omega} \right) \right)^2 \right)$$

All coefficients of the model are listed in Table 1. In order to achieve accurate and reliable results, the tools could make the mesh coarser or finer considering the input condition and the turbulence model. Details of domain mesh are presented in Table 1. Boundary layer mesh is used to satisfy y^+ criteria. Domain mesh is shown in Fig. 9.

Table 1. Blade-to-blade domain mesh.

Boundary	Grid number	Grid property
Inlet periodic	101	Grid ratio is 1.02
Inlet	51	Grid ratio is 1
Blade walls	101	Grid ratio is 1.02 double
Outlet periodic	91	Grid ratio is 1.02
Leading and trailing edges	5	Grid ratio is 1
Boundary layer	10	First row height is 0.01(mm) and growth factor is 1.25

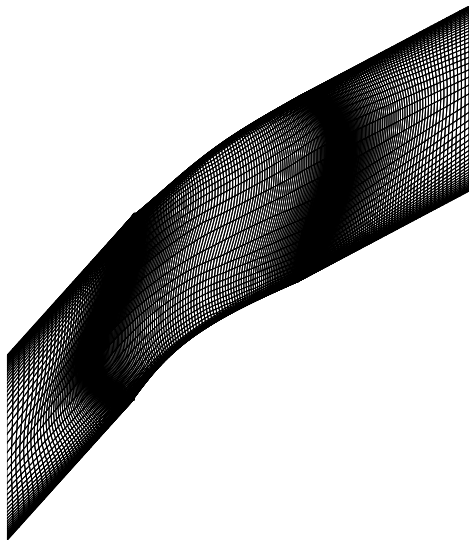


Fig. 9. Cascade domain mesh.

The surface pressure coefficient (Eq. (14)) distributions at design point conditions resulting from the experimental cascade tests [16] and Navier-Stokes solver calculations for a controlled diffusion blade are shown in Fig. 10.

$$C_p = \frac{p - p_1}{0.5\rho V^2} \quad (14)$$

A good agreement between the experimental data and those simulated by the presented flow

solver is observed. This agreement is pronounced along the whole blade surfaces. Therefore, the comparison indicated that the present flow solver has enough accuracy to be used in this work.

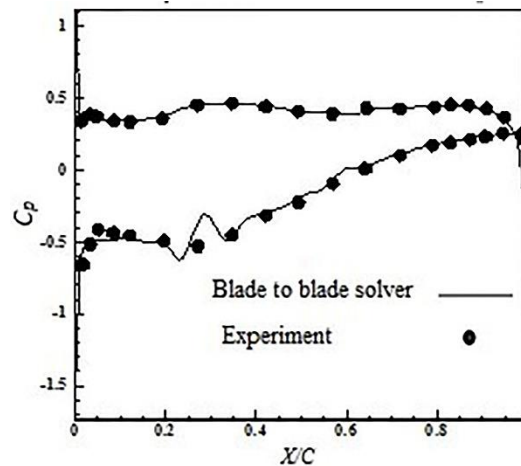


Fig. 10. Pressure coefficient over blade surfaces comparing the experimental [13] and numerical results.

4. Results and discussion

The objective of the airfoil design is turning the flow to create lift power with the least loss in static pressure. The loss is usually created as a result of a lack of balance between input and output pressures and shear forces between the fluid and the airfoil. Both loss generating mechanisms are affected by the boundary layer beside the wall. Blade design affects the development of the boundary layer via three methods. The first one is the positive pressure gradient on the suction surface of the blade which causes the flow separation on suction surface. The second one is the intense variations of the surface curvature in leading edge which causes the creation of local separation on the attack edge. The third one is the shape of the pressure surface due to the creation of high-pressure areas on the pressure surface. In leading edge, the designer can define the surface curvature without intense variations on the curvature near pressure and suction surfaces. Therefore, the designer can control the growth of the boundary layer by optimization of the curvature of the surfaces.

In this paper, three different methods are presented to optimize the blades of an axial flow compressor. The optimization of these blades aims to reduce the loss in the design angle of attack and increase the permitted range of angle of attack. Therefore, weight coefficients of the objective function are considered to be $\omega_1=0.4$, $\omega_2=0.2$, and $\omega_3=0.4$. In all three methods, input and output angles, installation angle, and the proportion of the chord length to the distance among blades are considered to be equal to the primary blade. A double circular arc (DCA) blade is used as the primary guess in each of the three methods. The quality of the optimized blade is achieved by each method through comparing the performance of the blade with the initial blade. The results provided in Tables 2, 3, and 4 show that the greatest reduction in the design point loss coefficient and the greatest increase in the allowable range of the angles of attack are associated with the optimized blade using the first method. Reduction in the loss in the second method is more than the third method; however, increase in the range of allowable angles of attack is inconsiderable in these two methods.

Table 2. Performance comparison between DCA and optimized blade in first method

	Initial	Design	Change (%)
ω_{min}	3.98	3.38	-15.07
$\Delta\alpha$	16	18.84	17.75
CL	0.79	0.78	-0.89
CPU Time	16 hours		

Table 3. Performance comparison between DCA and optimized blade in second method.

	Initial	Design	Change (%)
ω_{min}	3.98	3.49	-12.31
$\Delta\alpha$	16	16.24	1.5
CL	0.79	0.79	0
CPU Time	17 hours & 30 minutes		

Table 4. Performance comparison between DCA and optimized blade in third method.

	Initial	Design	Change (%)
ω_{min}	3.98	3.65	-8.29
$\Delta\alpha$	16	16.4	2.5
CL	0.79	0.79	0
CPU Time	17 hours & 30 minutes		

In Fig. 11(a), the geometry of the blade optimized by the first method and the DCA blade is compared. The inlet and outlet angles of both blades are the same, but the camber line of the optimized blade is very different from that of the first blade. Fig. 11(b) shows the comparison of the curvature distribution of pressure and suction surfaces and camber line for optimized blade and the initial blade. In DCA blade, the highest value of curvature is in the middle of the blade surface (blade with middle loading); therefore, flow acceleration on the pressure surface is carried out in the middle of the blade. However, in the optimized blade, the maximum curvature and, consequently, the maximum loading of the flow is at the beginning of the suction surface (blade with initial loading). In the optimized blade, the curvature of the suction surface steadily decreases from leading edge up to trailing edge. Therefore, the flow accelerates at the beginning of the blade, and the boundary layer of the flow becomes turbulent, but the possibility of flow separation along the suction surface decreases. Fig. 11(b) shows, the thickness of the boundary layer in the leading edge of the optimized blade is less than that of the primary blade. In minus off-design angles of attack, the fluid flow accelerates at the attack edge. In the optimized blade, the acceleration of the attack edge along with the acceleration of the beginning of the suction surface causes the acceleration of the transition of laminar to turbulent flow; however, in the rest of the suction surface, the possibility of rapid growth and flow separation is low. In DCA blade, the leading edge causes the flow transition from laminar to turbulent, but the acceleration of the flow in the middle of the suction surface causes rapid growth or flow separation. As shown in Fig. 11(c), the allowed minus angle in the optimized blade is far less than that in the primary blade. Blade optimization using the second method causes 12% reduction in the loss coefficient in design angle of attack, but the allowable operation range of the angles of attack has no considerable change compared with the primary blade.

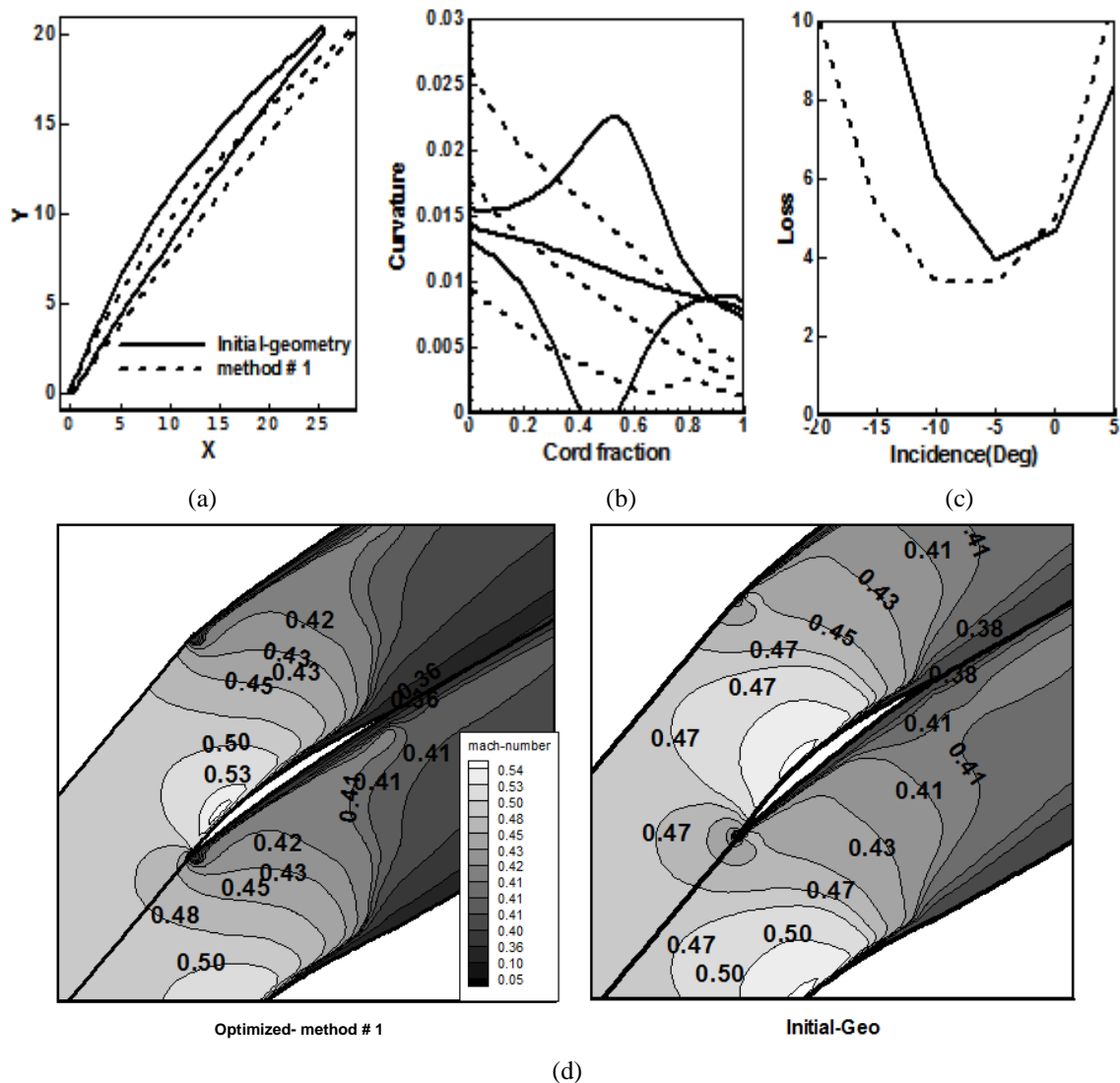


Fig. 11. Comparison between DCA (solid line) and optimized blade in first method (dashed line), a: Blade geometry, b: Curvature variation along the chord, c: Loss variation versus incidence angle, d: Mach distribution.

Fig. 12 compares the geometry and the operation of the optimized blade using the second method with the primary blade. Fig. 12(a) shows the comparison between the geometry of the optimized blade and DCA blade. As shown in Fig. 12(b), the maximum curvature place in the optimized blade is a bit closer to leading edge rather primary blade. Therefore, the place of the maximum Mach number in this blade is closer to leading edge rather that of the primary blade. Fig. 12(d) shows that the flow accelerates at the beginning of this blade. The acceleration in the design angle of the attack causes the transition of flow from laminar to turbulent. Steady reduction

in curvature in the rest of the suction surface causes a small growth in the boundary layer in the suction surface. Therefore, the boundary layer's thickness at trailing edge in this blade is less than that of the primary blade (Fig. 12(d)). In off-design conditions, the leading edge causes flow transition from laminar to turbulent. The acceleration on the suction surface causes rapid growth of the boundary layer or flow separation at this point. In view of Fig. 12(c), blade operation in off-design conditions does not have a significant improvement compared with DCA blade.

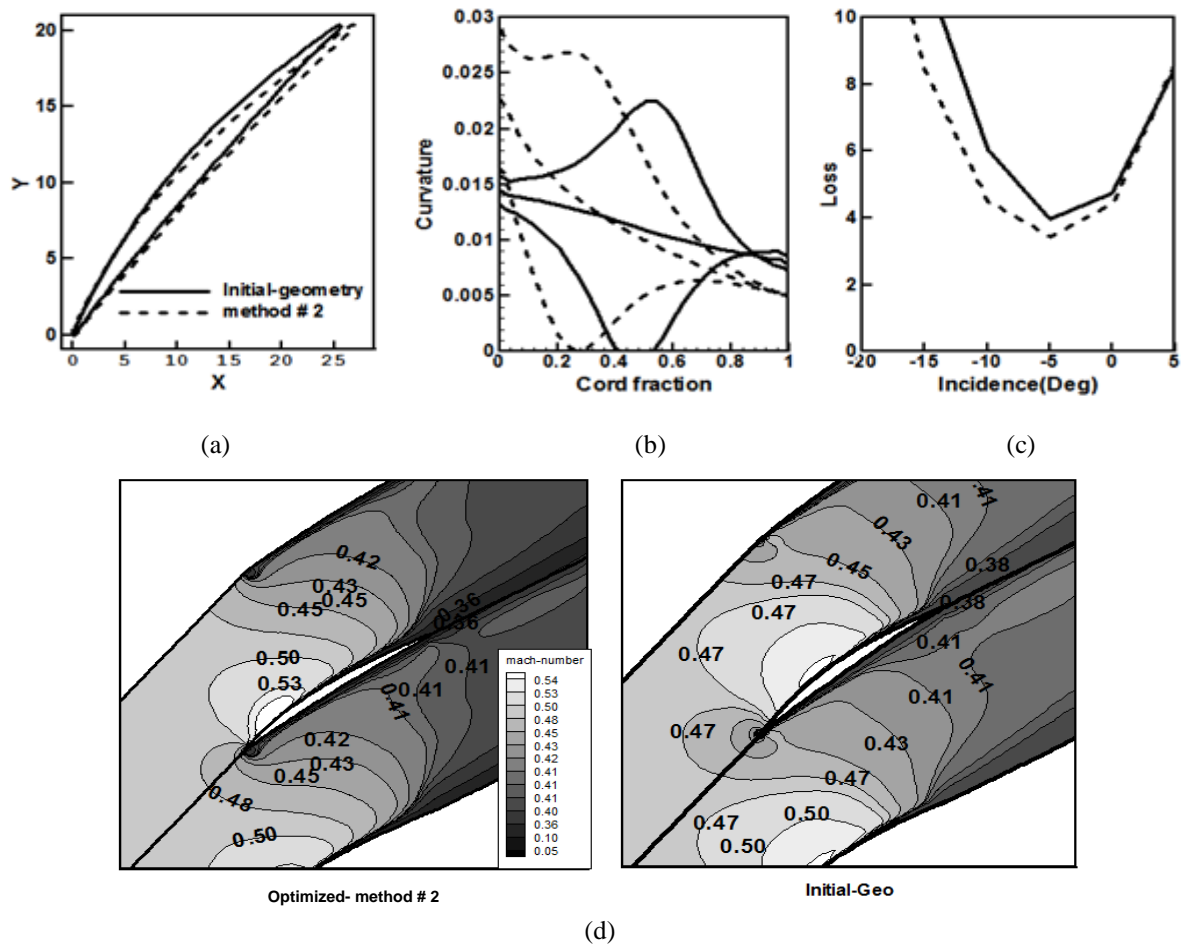


Fig. 12. Comparison between DCA (solid line) and optimized blade in second method (dashed line), a: Blade geometry, b: Curvature variation along the chord, c: Loss variation versus incidence angle, d: Mach distribution.

Fig. 13 compares the geometry and performance of the blade optimized using the third method with the primary blade. Fig. 13(a) shows the curvature of the optimized blade which has no considerable changes compared with the primary blade. In the blade optimized using this method, the maximum curvature value is transferred to the beginning of the blade.

Table 2 provides that the number of parameters of the third method is much smaller than that of the other two methods; the optimization time in this method is almost 2.5 times less. However, the maximum curvature of this blade is great compared with that of the primary blade. As shown in Fig. 13(d), the place of the maximum Mach is transferred to the beginning of the blade. Therefore, in design angle, the loss

coefficient has 8% reduction compared with that of the primary blade. In off-design circumstances, the blade operation has no significant improvement because the high curvature of the beginning of the suction surface and the primary acceleration of the flow in attack edge cause rapid growth or separation of the boundary layer in this area. Fig. 13(c) compares the loss curve of the optimized blade and that of the primary blade. However, the reduction in the number of parameters causes the flexibility of blade geometry to decrease in the optimization process; consequently, the improvement in the blade performance is less than that of the other two methods. The number of parameters in the first method is more than that of the second method, but its optimization time is less.

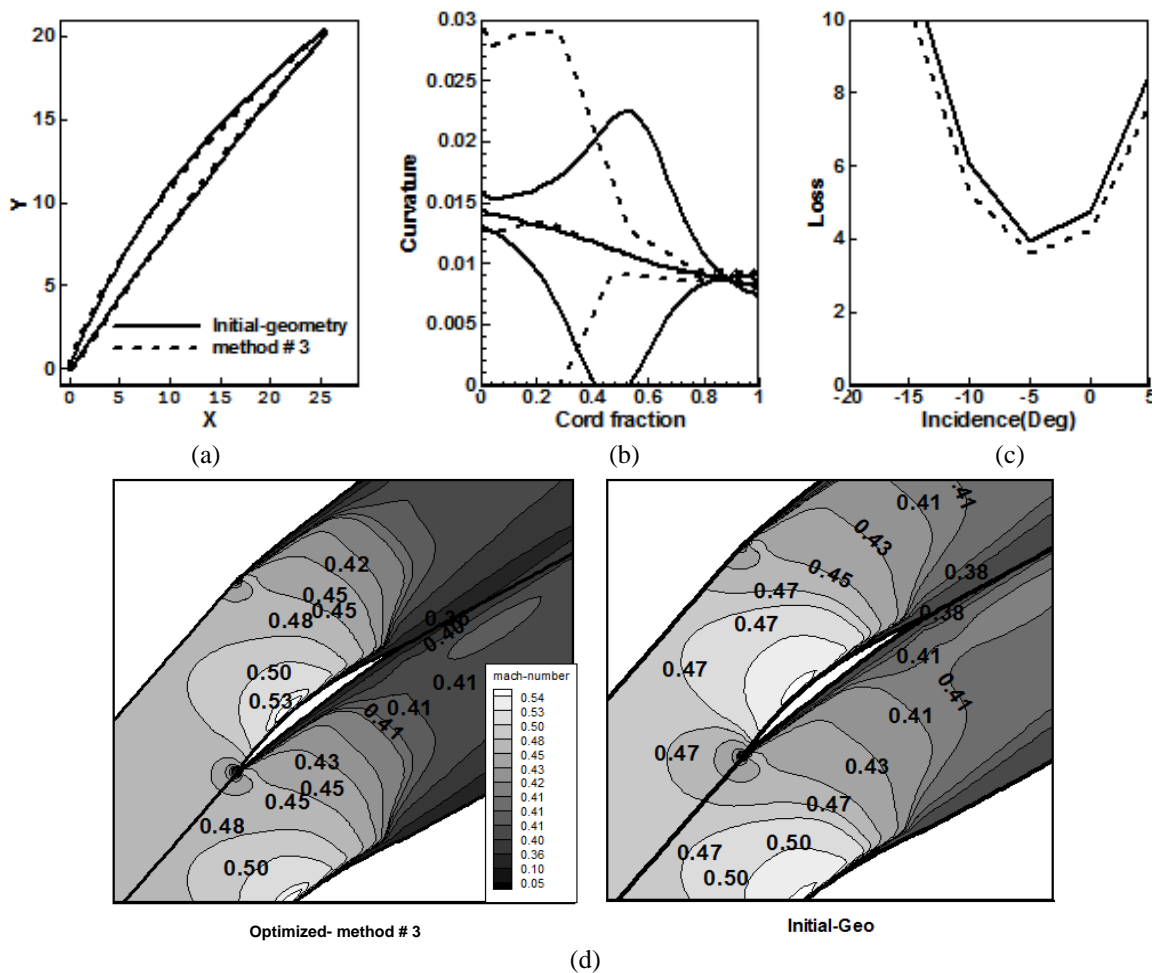


Fig. 13. Comparison between DCA (solid line) and optimized blade in third method (dashed line), a: Blade geometry, b: Curvature variation along the chord, c: Loss variation versus incidence angle, d: Mach distribution.

Using geometrical parameters, which have a close relationship with the flow pattern on the blade (such as surface curvature which is associated with the distribution of Mach number and the boundary layer growth [9]) causes the optimization time in the first method to decrease. Therefore, the numbers and types of design parameters have a great impact on the time and quality of blade optimization.

5. Conclusions

The present study presents three different methods for multiple-point optimization of the axial flow compressor blades. DCA blade is used in all three methods as the primary guess. The first method has the highest number of

parameters and, after that, the second and third methods have the highest number of parameters, respectively. The most performance improvement is related to the first method with 15% reduction in the loss coefficient of the design angle of attack and 17% increase in the allowed range of performance. The optimization of all three blades caused a transfer of the maximum curvature of surfaces from the middle to the front of the blade. In the first method, in which the tool of blade generation is more flexible, the maximum curvature is less, and it is at the beginning of the suction surface. In this method, despite more design parameters compared with the second method, the optimization time is less. The results show that

the use of geometrical parameters, which directly affect the flow pattern, has a great impact on the quality and time of optimization.

References

- [1] K. Park, M. G. Turner, K. Siddappaji, S. Dey, and A. Merchant, "Optimization of a 3-stage booster: part 1-the axisymmetric multi-disciplinary optimization approach to compressor design", in *ASME 2011 Turbo Expo: "Turbine Technical Conference and Exposition"*, pp. 1413-1422, (2011).
- [2] D. Bonaiuti and M. Zangeneh, "On the coupling of inverse design and optimization techniques for the multiobjective, multipoint design of turbomachinery blades", *Journal of Turbomachinery*, Vol. 131, No. 2, p. 021014, (2009).
- [3] T. Korakianitis, "Hierarchical development of three direct-design methods for two-dimensional axial-turbomachinery cascades", *Journal of turbomachinery*, Vol. 115, No. 2, pp. 314-324, (1993).
- [4] T. Sonoda, Y. Yamaguchi, T. Arima, M. Olhofer, B. Sendhoff, and H.-A. Schreiber, "Advanced High Turning Compressor Airfoils for Low Reynolds Number Condition: Part 1-Design and Optimization", in *ASME Turbo Expo 2003, "collocated with the 2003 International Joint Power Generation Conference"*, pp. 437-450, (2003).
- [5] S. Shahpar and D. Radford, "Application of the FAITH linear design system to a compressor blade", *International Society for Air Breathing Engines- ISOABE, "ISABE- International Symposium on Air Breathing Engines"*, 14 th, Florence, Italy, (1999).
- [6] S. Kammerer, J. Mayer, M. Paffrath, U. Wever, and A. Jung, "Three-dimensional optimization of turbomachinery bladings using sensitivity analysis", in *ASME Turbo Expo 2003, "collocated with the 2003 International Joint Power Generation Conference"*, pp. 1093-1101, (2003).
- [7] D. Buche, G. Guidati, and P. Stoll, "Automated design optimization of compressor blades for stationary, large-scale turbomachinery", in *ASME Turbo Expo 2003, "collocated with the 2003 International Joint Power Generation Conference"*, pp. 1249-1257, (2003)
- [8] E. Benini and A. Tournlidakis, "Design optimization of vaned diffusers of centrifugal compressors using genetic algorithms", *15th AIAA Computational Fluid Dynamics Conference*, Vol. 2583, pp. 2001, (2001).
- [9] D. Bonaiuti and V. Pediroda, "Aerodynamic optimization of an industrial centrifugal compressor impeller using genetic algorithms", in *Proceedings of Eurogen*, pp. 467-472, (2001).
- [10] K. Siddappaji, M. G. Turner, S. Dey, K. Park, and A. Merchant, "Optimization of a 3-Stage Booster: Part 2-The Parametric 3D Blade Geometry Modeling Tool", in *ASME 2011 Turbo Expo: "Turbine Technical Conference and Exposition"*, pp. 1431-1443, (2011).
- [11] R. Jaron, A. Moreau, S. Gu erin, and R. Schnell, "Optimization of Trailing-Edge Serrations to Reduce Open-Rotor Tonal Interaction Noise", *Journal of Fluids Engineering*, Vol. 140, No. 2, pp. 021201-021201-8, (2017).
- [12] S. Vitale, T. A. Albring, M. Pini, N. R. Gauger, and P. Colonna, "Fully turbulent discrete adjoint solver for non-ideal compressible flow applications", *Journal of the Global Power and Propulsion Society*, Vol. 1, pp. 252-270, (2017).
- [13] H. Schreiber and H. Starcken, "Experimental cascade analysis of atransonic compressor rotor blade section", *Journal of Engineering for Gas Turbines and Power*, Vol. 106, No. 2, pp. 288-294, (1984).
- [14] M. Kermani and E. Plett, "Modified entropy correction formula for the Roe scheme", *39th Aerospace Sciences Meeting and Exhibit*, (2001).

- [15] B. Van Leer, "Towards the ultimate conservative difference scheme. V. A second-order sequel to Godunov's method", *Journal of computational Physics*, Vol. 32, No. 1, pp. 101-136, (1979).
- [16] W. Steinert, B. Eisenberg, and H. Starken, "Design and testing of a controlled diffusion airfoil cascade for industrial axial flow compressor application", *Journal of Turbomachinery*, Vol. 113, No. 4, pp. 583-590, (1991).

How to cite this paper:

Omid Fathi and Hadi Kargarsharifabad, "Presenting three design methods for axial compressor blade via optimization" *Journal of Computational and Applied Research in Mechanical Engineering*, Vol. 8, No. 1, pp. 107-120, (2018).

DOI: 10.22061/jcarme.2018.1948.1164

URL: http://jcarme.sru.ac.ir/?_action=showPDF&article=770

